Nonfrustrated Interlayer Order and its Relevance to the Bose-Einstein Condensation of Magnons in $BaCuSi_2O_6$

Vladimir V. Mazurenko,[1,*] Maria V. Valentyuk,[1,2] Raivo Stern,[3,†] and Alexander A. Tsirlin[3,‡]
[1]*Theoretical Physics and Applied Mathematics Department, Ural Federal University, 620002 Ekaterinburg, Russia*
[2]*Institute of Theoretical Physics, University of Hamburg, Jungiusstraße 9, 20355 Hamburg, Germany*
[3]*National Institute of Chemical Physics and Biophysics, 12618 Tallinn, Estonia*
(Received 25 September 2013; revised manuscript received 21 January 2014; published 10 March 2014)

Han purple ($BaCuSi_2O_6$) is not only an ancient pigment, but also a valuable model material for studying Bose-Einstein condensation of magnons in high magnetic fields. Using precise low-temperature structural data and extensive density-functional calculations, we elucidate magnetic couplings in this compound. The resulting magnetic model comprises two types of nonequivalent spin dimers, in excellent agreement with the ^{63,65}Cu nuclear magnetic resonance data. We further argue that leading interdimer couplings connect the upper site of one dimer to the bottom site of the contiguous dimer, and not the upper-to-upper and bottom-to-bottom sites, as assumed previously. This finding is verified by inelastic neutron scattering data and implies the lack of frustration between the layers of spin dimers in $BaCuSi_2O_6$, thus challenging existing theories of the two-dimensional-like Bose-Einstein condensation of magnons in this compound.

DOI: 10.1103/PhysRevLett.112.107202 PACS numbers: 75.10.Jm, 05.30.Jp, 75.30.Et, 75.50.Ee

Bose-Einstein condensation (BEC), one of the basic phenomena in quantum physics, has long remained elusive in experiments until the condensation of bosons in ultracold atomic gases was observed [1]. More recently, gapped quantum magnets opened another direction in the experimental studies of BEC [2]. Here, individual electronic spins form dimers that can be either in a singlet ($S = 0$) or in a triplet ($S = 1$) state. The singlet ground state leads to a quantum spin liquid with gapped magnetic excitations, as typical for dimerized spin-$\frac{1}{2}$ magnets. An external magnetic field pushes the triplet state (effective boson) down in energy, so that it eventually becomes populated. Above a certain critical field H_{c1}, the concentration of triplets (the chemical potential of bosons) departs from zero, and the system undergoes a BEC transition that manifests itself by a field-induced magnetic ordering observed in thermodynamic measurements [3,4], neutron scattering [5], and nuclear magnetic resonance (NMR) [6,7] experiments.

The BEC of magnons has been observed and extensively investigated in several model magnetic materials, including $BaCuSi_2O_6$ [4,7–11] and $TlCuCl_3$ [3,5,6]. In contrast to cold atomic gases, where the spatial arrangement of bosons and their interactions are determined by the external potential, bosonic systems in quantum magnets are to a large extent predefined by particular crystal structures and ensuing electronic interactions. For example, in $BaCuSi_2O_6$ an unconventional critical exponent reminiscent of a two-dimensional (2D) behavior in an outwardly three-dimensional (3D) spin system has been ascribed to a peculiar pattern of frustrated (competing) interactions between the magnetic layers [9,12]. The magnetic frustration decouples individual layers, thus leading to a dimensional reduction at the quantum critical point at H_{c1}, where the spin-liquid phase borders the long-range-ordered BEC phase [9].

Later studies of $BaCuSi_2O_6$ amended this interesting picture by reporting a low-temperature structural distortion that splits the uniform spin lattice of $BaCuSi_2O_6$ into magnetic layers of two different types [7,13,14]. However, all experimental [9,11] and theoretical [12,15–17] studies available so far consider frustration of interlayer interactions as an integral part of $BaCuSi_2O_6$. Here, we challenge this well-established paradigm by evaluating individual magnetic couplings in $BaCuSi_2O_6$ from density-functional (DFT) calculations and reanalyzing the neutron-scattering data. We find that $BaCuSi_2O_6$ is essentially a nonfrustrated magnet, at least on the level of isotropic interactions of the Heisenberg model, and suggest that the mechanism of the 2D-like magnon BEC in this compound should be reconsidered.

$BaCuSi_2O_6$ is colloquially known as Han purple, the pigment used in ancient China [18]. Its room-temperature crystal structure, although unknown to the original Chinese users, is tetragonal (space group $I4_1/acd$) and features CuO_4 square plaquettes connected via Si_4O_{10} ring units of corner-sharing SiO_4 tetrahedra (Fig. 1) [19]. The plaquettes are linked in such a way that two Cu atoms are separated by 2.75 Å only, forming a well-defined structural and magnetic dimer. The dimers are arranged into slabs, thus forming magnetic bilayers (Fig. 1). It is commonly believed that the in-plane order is antiferromagnetic (AFM), driven by the coupling J_{ab}.

The bilayers are interleaved by Ba^{2+} cations. The stacking of the bilayers is such that each spin-$\frac{1}{2}$ Cu^{2+} ion interacts with four Cu^{2+} ions of the neighboring layer,

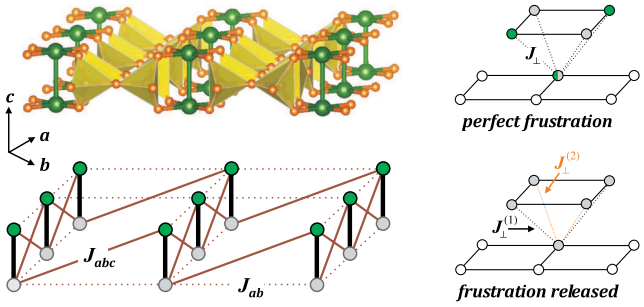

FIG. 1 (color online). Left panel: crystal structure of the magnetic bilayer and the relevant magnetic model with the FM in-plane order driven by the AFM interdimer coupling $J_{abc} \gg J_{ab}$. Green (dark) and gray (light) circles denote different spin directions. Right panel: different regimes of the interlayer order depending on the in-plane magnetic order. The AFM in-plane order leads to a perfect frustration (top). The FM in-plane order lifts the frustration (bottom). $J_\perp^{(1)}$ and $J_\perp^{(2)}$ are two different interlayer couplings in the low-temperature structure of $BaCuSi_2O_6$. Both are weak and FM. Crystallographic plots are done using the VESTA software [20].

two of them having one spin direction and the other two having an opposite spin direction, because the in-plain order is, presumably, AFM (Fig. 1, top right). This way, the interlayer couplings $J_\perp$ are perfectly frustrated, no matter whether $J_\perp$ is ferromagnetic (FM) or AFM. While these coupling are very weak, likely below 1 K [4,13], their allegedly frustrated nature prevents the system from a 3D ordering. This crucial microscopic feature underlies the idea of the dimensional reduction at the QCP and the current understanding of the 2D-like BEC in $BaCuSi_2O_6$. However, the frustrated nature of $J_\perp$ is invalidated by our detailed microscopic analysis reported below.

In the following, we evaluate individual magnetic couplings in $BaCuSi_2O_6$ using DFT band-structure calculations performed in the FPLO [21] code. From a tight-binding analysis of the band structure calculated on the level of local density approximation, we obtain hopping integrals t_i that are related to AFM exchange integrals as $J_i^{\mathrm{AFM}} = 4t_i^2/U_{\mathrm{eff}}$, where U_{eff} is an effective on-site Coulomb repulsion in the Cu $3d$ shell. Alternatively, we estimate exchange couplings J_i as energy differences between collinear FM and AFM spin configurations calculated within the generalized gradient approximation (GGA) + U approach, where the Hubbard U parameter accounts for electronic correlation in a mean-field fashion. We have cross-checked the above FPLO results using total-energy calculations in the VASP code [22] and the Lichtenstein exchange integral procedure [23] implemented in TB-LMTO-ASA [24]. All these approaches provide the consistent microscopic scenario of $BaCuSi_2O_6$ [25].

We start with the room-temperature $I4_1/acd$ structure of $BaCuSi_2O_6$ (Table I). Here, both t_i and J_i support the overall model of spin dimers forming the bilayers.

TABLE I. Magnetic couplings in the high-temperature and low-temperature phases of $BaCuSi_2O_6$: Cu-Cu distances d (in Å), transfer integrals t_i (in meV), and exchange integrals J_i (in K). Note that the t_i values represent AFM contributions to the exchange, according to $J_i^{\mathrm{AFM}} = 4t_i^2/U_{\mathrm{eff}}$, where U_{eff} is the effective on-site Coulomb repulsion. Full exchange couplings J_i are obtained from GGA + U with $U_d = 8.5$ eV, $J_d = 1$ eV and the fully localized limit double-counting correction [26].

	J	J_{ab}	J_{abc}	$J_\perp$
d	2.75	7.08	7.59	5.77
t	−93	−2	36	−5
J	53	−0.4	7.9	−0.3

	J^A	J^B	J^A_{ab}	J^B_{ab}	J^A_{abc}	J^B_{abc}	$J_\perp^{(1)}$	$J_\perp^{(2)}$
d	2.70	2.78	7.04	7.04	7.54	7.57	5.73	5.72
t	−88	−105	2	−10	33	38	−4	−5
J	52	65	−0.3	−0.3	7.7	7.8	−0.2	−0.3

However, we find that the leading interdimer couplings within the bilayer is clearly J_{abc} and not J_{ab}. The upper site of one dimer is coupled to the bottom site of the neighboring dimer, thus leading to the FM in-plane order. This FM order lifts the frustration of $J_\perp$ (Fig. 1).

The unexpected $J_{abc} \gg J_{ab}$ coupling regime can be rationalized by considering individual atomic orbitals that contribute to the electron hopping and, therefore, to the superexchange process. Figure 2 shows Wannier functions based on the Cu $3d_{x^2-y^2}$ orbitals. Each Wannier function comprises $p\sigma$ contributions of four nearest-neighbor oxygen atoms O1 and O3 (about 10% each) and, additionally, four smaller contributions of second-neighbor oxygens O2 (about 0.5% each). These second-neighbor contributions are not unusual and largely determine the superexchange in Cu^{2+}magnets [27]. In $BaCuSi_2O_6$, the superexchange follows the Cu-O1-O2-O3-Cu pathway and, therefore, crucially depends on the O1-O2-O3 angle, which is 95.5° for J_{ab} and 156.1° for J_{abc}. Therefore, J_{abc} should be the leading interdimer coupling because of the more favorable orbital overlap according to the conventional Goodenough-Kanamori-Anderson rules [28].

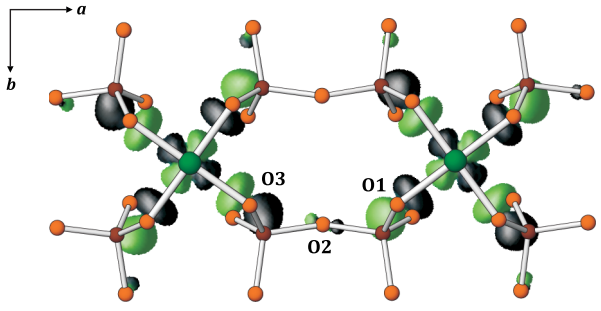

FIG. 2 (color online). Cu-based Wannier functions showing the mechanism of the Cu-O1-O2-O3-Cu superexchange in $BaCuSi_2O_6$.

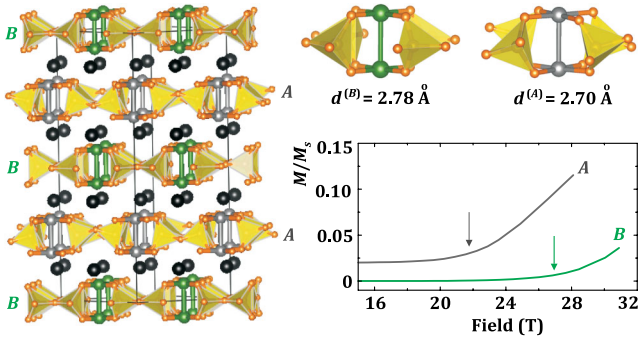

FIG. 3 (color online). Low-temperature orthorhombic structure of $BaCuSi_2O_6$ with two inequivalent dimers A and B. Bottom right part shows the simulated magnetization curves of individual bilayers at $T/J = 0.05$. The arrows mark the critical fields of $H_{c1}^{(A)} \simeq 22$ T and $H_{c1}^{(B)} \simeq 27$ T, where the relevant spin gaps are closed.

Let us now consider the changes in the magnetic model upon the transition to the low-temperature orthorhombic *Ibam* structure around 100 K [14]. Here, tiny alterations in the mutual arrangement of the CuO_4 and SiO_4 units render two neighboring bilayers inequivalent (Fig. 3). These bilayers labeled A and B feature different intradimer couplings, as seen by the inelastic neutron scattering (INS) [13] and NMR [7]. Indeed, we find two types of the intradimer exchange J^A and J^B (Table I). All other couplings also split into two, but only J^A and J^B reveal a sizable difference. The interdimer exchange remains largely unchanged, so that the $J_{abc} \gg J_{ab}$ regime persists at low temperatures.

The structural difference between the A and B dimers is well seen in the Cu-Cu distances that are 2.70 and 2.78 Å, respectively. Surprisingly, we find that the AFM exchange is stronger for the longer Cu-Cu distance (J^B) and weaker for the shorter Cu-Cu distance (J^A), although a naive picture of the direct d-d overlap should be exactly the opposite. This unexpected result should be traced back to the nature of interacting orbitals visualized by the Cu-based Wannier functions in Fig. 2. The relevant orbitals lie in the CuO_4 plane, thus making the direct d-d exchange impossible. The intradimer coupling follows the long Cu-O1-O2-O3-Cu superexchange pathway instead, similar to the case of J_{abc}. Therefore, the intradimer exchange $J^{A,B}$ lacks any simple relation to the Cu-Cu distance $d^{A,B}$.

The emergence of a weaker coupling in the shorter Cu-Cu dimer is independently confirmed by the ^{63,65}Cu NMR experiments [7]. Here, the A and B dimers are distinguished according to their different spin gaps and different quadrupolar frequencies on the respective Cu sites. The B dimer with the larger spin gap (i.e., the stronger intradimer coupling) shows the smaller EFG, and the other way around. To verify that the strongly coupled B dimer is indeed the one with the longer Cu-Cu distance, we calculated the quadrupolar frequencies of 33.8 and 30.5 MHz for the A and B dimers, respectively. These values should be compared with 14.85 and 14.14 MHz from the NMR experiment [7]. While the absolute values of the quadrupolar frequencies are substantially overestimated and reflect well-known shortcomings of DFT in evaluating subtle features of charge distribution and electric field gradients, the qualitative effect of the smaller frequency on the stronger dimer is well reproduced. Therefore, the DFT and NMR results are in good agreement.

We can further make a quantitative comparison to the experiment. INS studies [13] yield $J^A \simeq 50$K and $J^B \simeq 55$ K in remarkable agreement with our DFT estimates listed in Table I. Regarding the interdimer exchange, Ref. [13] reports $J_{ab} \simeq 6$ K (AFM), whereas an earlier work [29] puts forward the FM coupling $J_{ab} \simeq -2.2$ K. This latter result supports our key finding of J_{abc} as the leading interdimer coupling. While J_{abc} is AFM, it leads to the FM order in the ab plane (Fig. 1) that can be seen as an effective FM coupling J_{ab} probed by the neutron scattering. In fact, the same conclusion is inferred from the data of Ref. [13]. The dispersion of the triplet band can be written as follows:

$$\varepsilon = J + (J_{ab} - J_{abc})[\cos(\pi h + \pi k) + \cos(\pi h - \pi k)], \quad (1)$$

which, considering the experimental dispersion [13,29], implies a positive J_{abc} (or negative J_{ab}, as in Ref. [29]). A positive $J_{ab} \gg J_{abc}$ would manifest itself by energy minima at odd h, in sharp contrast to the experimental dispersion showing the minima at even h, including $h = 0$ (Fig. 4, left). The different positions of the minima result from the fact that J_{ab} and J_{abc} lead to different ordering patterns in the ab plane (Fig. 1). The order established

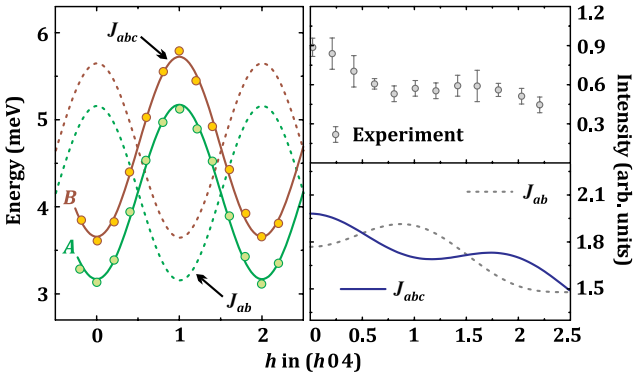

FIG. 4 (color online). Left panel: dispersions of the triplet bands corresponding to the A and B bilayers in $BaCuSi_2O_6$. Solid and dashed lines are drawn according to Eq. (1) for $J_{abc} \gg J_{ab}$ and $J_{ab} \gg J_{abc}$ regimes, respectively. Right panel: momentum dependence of the INS intensity (top) and the predictions of Eq. (2) for the $J_{abc} \gg J_{ab}$ (solid line) and $J_{ab} \gg J_{abc}$ (dashed line) scenarios (bottom). Experimental data from Ref. [13] are taken along the (h04) direction of the reciprocal space.

by J_{ab} is AFM, whereas J_{abc} would favor the FM in-plane order.

To calculate the scattering intensity, we used the single mode approximation [30]. In our case, $I(\mathbf{Q},\omega) = I(\mathbf{Q})\delta(\omega-\omega_{\mathbf{Q}})$, where $\omega_{\mathbf{Q}}$ is determined by Eq. (1). Therefore, we evaluate the intensities using the equation

$$I(\mathbf{Q}) \sim -|F(Q)|^2 \sum_{\mathbf{d}} A_{\mathbf{d}}[1-\cos(\mathbf{Qd})], \qquad (2)$$

where $\mathbf{d}$ are vectors connecting the Cu sites, $A_{\mathbf{d}} = J_{\mathbf{d}}\langle S_0 S_{\mathbf{d}}\rangle$, and for the sake of simplicity we consider the tetragonal $I4_1/acd$ crystal structure, because the effect of $J_{abc} \gg J_{ab}$ pertains to both polymorphs. The calculation for the relevant $\mathbf{Q}$ values shows that the model with $J_{abc} \gg J_{ab}$ reproduces the minimum of the intensity at $h \simeq 1$ (Fig. 4, right). In contrast, the model with $J_{abc} \ll J_{ab}$ will lead to a maximum at $h = 1$ in apparent contradiction to the experiment [31]. Therefore, the INS data strongly support the proposed microscopic magnetic model with $J_{abc} \gg J_{ab}$.

Our computed exchange couplings also reproduce the critical fields H_{c1} of individual bilayers, as shown by the magnetization isotherms calculated with the quantum Monte Carlo (QMC) algorithm implemented in the ALPS code [32]. The departure of the magnetization from zero signifies the closing of the spin gap. We find $H_{c1}^{A} \simeq 22$T and $H_{c1}^{B} \simeq 27$ T to be compared with $H_{c1} \simeq 23.4$ T obtained experimentally [7]. This critical field corresponds to the BEC transition in the A bilayer with the smaller spin gap. The interbilayer coupling generates triplets (bosons) in the B bilayer as well, even though the spin gap of this bilayer is not yet closed at H_{c1} [7]. This effect, which is arguably the most peculiar feature of $BaCuSi_2O_6$ relating to the dimensional reduction at the QCP, has been a matter of substantial theoretical interest [15–17].

The boson density in the bilayer B, $n_B(H)$, can be accessed with NMR. Its field dependence is presently understood in the framework of frustrated interlayer couplings (Fig. 1, right). The role of frustration is to impede the formation of bosons in the B bilayers, because boson densities exceeding experimental values are obtained when no frustration is involved (as in our model) [11]. On the other hand, the ideal frustration driven by four equivalent couplings $J_\perp$, as in the top right panel of Fig. 1, would be too strong and underestimates the experimental densities. The "partial frustration" introduced by two inequivalent couplings $J_\perp^{(1)}$ and $J_\perp^{(2)}$ (Fig. 1, bottom right) [16] seemingly solves this problem and adjusts the calculated boson density close to the experimental values [11]. However, our reevaluation of $BaCuSi_2O_6$ puts forward the essential fact that there is the FM in-plane order and, hence, no appreciable frustration of the interlayer couplings, no matter whether $J_\perp^{(1)}$ and $J_\perp^{(2)}$ are equal or not. This holds as long as $J_\perp^{(1)}$ and $J_\perp^{(2)}$ are of the same sign, which is the case in $BaCuSi_2O_6$ (Table I).

We suggest that other sources of the magnetic frustration or even other explanations of the 2D-like magnon BEC in $BaCuSi_2O_6$ should be considered. Our results exclude any appreciable frustration on the level of isotropic exchange couplings (Heisenberg model). Magnetic anisotropy will in some cases introduce frustration, and the possibility of Dzyaloshinsky-Moriya interactions within the A bilayers may be important in this respect [14]. An alternative interpretation involves more than two types of inequivalent bilayers with different spin gaps that will then naturally affect the formation of bosons above H_{c1}. The signatures of an incommensurate structural modulation at low temperatures [33] and a complex shape of dimer excitations reported in Ref. [13] are pointing toward this scenario. However, further experimental input is required to analyze the magnetic anisotropy and structural details and eventually understand the BEC transition in $BaCuSi_2O_6$ theoretically.

In summary, we have analyzed magnetic couplings in $BaCuSi_2O_6$ and found that the diagonal interdimer coupling J_{abc} and the ensuing FM in-plane order should be basic ingredients of the magnetic model. The interbilayer coupling is about -0.2 K only, but it does not prevent and rather facilitates the 3D magnetic order. Our model is in excellent agreement with the zero-field neutron data, yet it does not fully explain peculiarities of the boson density right above the BEC transition. Frustration of interlayer couplings that was earlier speculated as a crucial feature of $BaCuSi_2O_6$ and the main origin of the 2D-like magnon BEC is in fact completely irrelevant to this compound. We conclude that $BaCuSi_2O_6$, a seemingly well-known model BEC material, still keeps a lot of puzzles that require further investigation.

The work of V. V. M. and M. V. V. was supported by the grant program of President of Russian Federation MK-5565.2013.2, the contracts of the Ministry of Education and Science of Russia N 14.A18.21.0076 and 14.A18.21.0889. A. T. acknowledges financial support from the ESF via the Mobilitas program (Grant No. MTT77). R. S. was funded by the Estonian Research Council (Grants No. ETF8440 and No. PUT210). We acknowledge essential discussions with Cristian Batista and Christian Rüegg as well as fruitful communication with Frédéric Mila, Nicolas Laflorencie, Vladimir I. Anisimov, and Alexander I. Lichtenstein.

*mvv@dpt.ustu.ru
†raivo.stern@kbfi.ee
‡altsirlin@gmail.com

[1] M. H. Anderson, J. R. Ensher, M. R. Matthews, C. E. Wieman, and E. A. Cornell, Science **269**, 198 (1995); K. B. Davis, M.-O. Mewes, M. R. Andrews, N. J. van Druten, D. S. Durfee, D. M. Kurn, and W. Ketterle, Phys. Rev. Lett. **75**, 3969 (1995).
[2] T. Giamarchi, C. Rüegg, and O. Tchernyshyov, Nat. Phys. **4**, 198 (2008).

[3] T. Nikuni, M. Oshikawa, A. Oosawa, and H. Tanaka, Phys. Rev. Lett. **84**, 5868 (2000); A. Oosawa, H. Aruga Katori, and H. Tanaka, Phys. Rev. B **63**, 134416 (2001).
[4] M. Jaime, V. F. Correa, N. Harrison, C. D. Batista, N. Kawashima, Y. Kazuma, G. A. Jorge, R. Stern, I. Heinmaa, S. A. Zvyagin, Y. Sasago, and K. Uchinokura, Phys. Rev. Lett. **93**, 087203 (2004).
[5] C. Rüegg, N. Cavadini, A. Furrer, H.-U. Güdel, K. Krämer, H. Mutka, A. Wildes, K. Habicht, and P. Vorderwisch, Nature (London) **423**, 62 (2003); C. Rüegg, B. Normand, M. Matsumoto, A. Furrer, D. F. McMorrow, K. W. Krämer, H. U. Güdel, S. N. Gvasaliya, H. Mutka, and M. Boehm, Phys. Rev. Lett. **100**, 205701 (2008).
[6] O. Vyaselev, M. Takigawa, A. Vasiliev, A. Oosawa, and H. Tanaka, Phys. Rev. Lett. **92**, 207202 (2004).
[7] S. Krämer, R. Stern, M. Horvatić, C. Berthier, T. Kimura, and I. R. Fisher, Phys. Rev. B **76**, 100406(R)(2007).
[8] S. E. Sebastian, P. A. Sharma, M. Jaime, N. Harrison, V. Correa, L. Balicas, N. Kawashima, C. D. Batista, and I. R. Fisher, Phys. Rev. B **72**, 100404(R) (2005).
[9] S. E. Sebastian, N. Harrison, C. D. Batista, L. Balicas, M. Jaime, P. A. Sharma, N. Kawashima, and I. R. Fisher, Nature (London) **441**, 617 (2006).
[10] S. A. Zvyagin, J. Wosnitza, J. Krzystek, R. Stern, M. Jaime, Y. Sasago, and K. Uchinokura, Phys. Rev. B **73**, 094446 (2006).
[11] S. Krämer, N. Laflorencie, R. Stern, M. Horvatić, C. Berthier, H. Nakamura, T. Kimura, and F. Mila, Phys. Rev. B **87**, 180405(R)(2013).
[12] C. D. Batista, J. Schmalian, N. Kawashima, P. Sengupta, S. E. Sebastian, N. Harrison, M. Jaime, and I. R. Fisher, Phys. Rev. Lett. **98**, 257201 (2007).
[13] C. Rüegg, D. F. McMorrow, B. Normand, H. M. Rønnow, S. E. Sebastian, I. R. Fisher, C. D. Batista, S. N. Gvasaliya, C. Niedermayer, and J. Stahn, Phys. Rev. Lett. **98**, 017202 (2007).
[14] D. V. Sheptyakov, V. Y. Pomjakushin, R. Stern, I. Heinmaa, H. Nakamura, and T. Kimura, Phys. Rev. B **86**, 014433 (2012); J. Schmalian and C. D. Batista, *ibid.* **77**, 094406 (2008).
[15] O. Rösch and M. Vojta, Phys. Rev. B **76**, 180401(R)(2007).
[16] O. Rösch and M. Vojta, Phys. Rev. B **76**, 224408 (2007).
[17] N. Laflorencie and F. Mila, Phys. Rev. Lett. **102**, 060602 (2009); **107**, 037203 (2011).
[18] H. Berke, Chem. Soc. Rev. **36**, 15 (2007).
[19] K. M. Sparta and G. Roth, Acta Crystallogr. Sect. B **60**, 491 (2004).
[20] K. Momma and F. Izumi, J. Appl. Crystallogr. **44**, 1272 (2011).
[21] K. Koepernik and H. Eschrig, Phys. Rev. B **59**, 1743 (1999).
[22] G. Kresse and J. Furthmüller, Comput. Mater. Sci. **6**, 15 (1996); **54**, 11169 (1996).
[23] A. I. Liechtenstein, M. I. Katsnelson, V. P. Antropov, and V. A. Gubanov, J. Magn. Magn. Mater. **67**, 65 (1987).
[24] O. K. Andersen, Z. Pawlowska, and O. Jepsen, Phys. Rev. B **34**, 5253 (1986).
[25] Our GGA $+ U$ calculations yield the band gap of about 3.2 eV and the magnetic moment of 0.82 μ_B on Cu atoms at $U_d = 8.5$eV and $J_d = 1$ eV.
[26] P. S. Berdonosov, O. Janson, A. V. Olenev, S. V. Krivovichev, H. Rosner, V. A. Dolgikh, and A. A. Tsirlin, Dalton Trans. **42**, 9547 (2013).
[27] A. A. Tsirlin, I. Rousochatzakis, D. Kasinathan, O. Janson, R. Nath, F. Weickert, C. Geibel, A. M. Läuchli, and H. Rosner, Phys. Rev. B **82**, 144426 (2010); A. A. Tsirlin, A. Möller, B. Lorenz, Y. Skourski, and H. Rosner, Phys. Rev. B **85**, 014401 (2012).
[28] P. W. Anderson, Solid State Phys. **14**, 99 (1963).
[29] Y. Sasago, K. Uchinokura, A. Zheludev, and G. Shirane, Phys. Rev. B **55**, 8357 (1997).
[30] M. B. Stone, W. Tian, M. D. Lumsden, G. E. Granroth, D. Mandrus, J.-H. Chung, N. Harrison, and S. E. Nagler, Phys. Rev. Lett. **99**, 087204 (2007).
[31] Here, we used $A = 1$ and $A_{ab} = 0.03$ in order to match the experimental data.
[32] A. F. Albuquerque *et al.*, J. Magn. Magn. Mater. **310**, 1187 (2007).
[33] E. C. Samulon, Z. Islam, S. E. Sebastian, P. B. Brooks, M. K. McCourt, Jr., J. Ilavsky, and I. R. Fisher, Phys. Rev. B **73**, 100407(R) (2006).